Indian Journal of Radio & Space Physics
Vol 42, June 2013, pp 150-158

Troposphere induced GPS navigation error, its effect on GPS-INS integrated system performance and mitigation strategies

G Harikumar[$,*], K Karthikeyan, S Syamala, C Radhakrishna Pillai, S Hemachandran[#], A Abdul Shukkoor & P P Mohanlal
ISRO Inertial Systems Unit, Thiruvananthapuram 695 013, India
E-mail: [$]harikumarganesan@yahoo.co.in, [#]s.heman@ieee.org

Received 7 November 2012; revised 28 March 2013; accepted 1 April 2013

Conventional Global Positioning System (GPS) receivers track GPS satellites above 5 degree horizon to avoid multipath effects. In order to improve vertical dilution of precision (VDOP), it is an attractive prospect to utilize GPS satellites below the horizon in addition to those above, for navigation computations in GPS receivers used by vehicles operating at high altitude trajectories. This paper, however, exposes a possible risk of navigation output degradation in adopting this scheme due to unintentional occultation of GPS signals from satellites below the earth tangent horizon. The error on GPS range and range rate measurements induced by troposphere are simulated using a model based approach. Results indicate position errors up to 150 m and velocity errors up to 14 ms^{-1} over a period of 15 s under practical conditions. Such slowly varying errors being uncharacteristic of GPS receivers are not rejected by the usual protection features in GPS-Inertial Navigation System (INS) integration schemes. Thereby, the integrated system performance is degraded. In the uncoupled GPS-INS scheme studied, GPS error of the above order resulted in integrated system output error of 100 m in position and 5 ms^{-1} in velocity, respectively. An altitude based elevation cut off scheme that can be incorporated in the GPS receiver for retaining the advantages of using negative elevation satellites, while avoiding occulted measurements, is presented in this paper. A method for strengthening integrated scheme protection, using innovation residuals, for rejecting such slow GPS errors is also presented.

Keywords: Global positioning system (GPS) navigation error, Inertial navigation system (INS), GPS signal occultation, Vertical dilution of precision (VDOP)

PACS Nos: *92.60.hf*; 84.40.Ua; 91.10.Fc

1 Introduction

Terrestrial GPS receivers used in standalone mode for real time navigation applications have to deal with multitude of error sources, viz. errors due to uncertainties in signal propagation (ionosphere and troposphere contributed errors); receiver noise and multipath; and control segment errors[1] (satellite clock and ephemeris model errors). While dual frequency measurements can eliminate most of the ionospheric error contributions, tropospheric effects are attempted to be compensated by adopting suitable models. Also, such receivers generally utilize signals from GPS satellites at an elevation of 5 deg from horizon and above for navigation computations, so that the multipath errors are minimized. This offers the added benefit of having lower tropospheric modeling errors (especially zenith delay – mapping function models) too. The control segment errors are bound to remain in standalone mode, but its range error contribution is of the order of 3 to 4 m (Ref. 1), which is acceptable for a number of applications. Once, the individual error contributions are dealt with, the positioning performance of the receiver largely depends on the position dilution of precision (PDOP). While it is routinely possible to get low horizontal dilution of precision (HDOP) with a good azimuthal coverage of satellites that are not too high above the horizon, owing to the elevation cut-off angle of 5 deg, the vertical dilution of precision (VDOP) is often higher[1].

However, GPS receivers operating at high altitude trajectories do not face the possibility of multipath errors provided the antennae are suitably placed on the vehicle. This presents an opportunity to avoid the elevation cut-off, thereby, gaining on the VDOP front. However, this comes with a cost: the signals from the negative elevation (w.r.t. local horizontal at the receiver) GPS satellites may traverse the earth's atmosphere and introduce measurement errors. While dual frequency measurements can again be leveraged to eliminate most of the ionospheric errors, the errors due to troposphere remain, and they cannot be compensated with usual tropospheric models used in terrestrial receivers. This condition occurs when the measurements are from a negative elevation GPS satellite, which is near/below the earth tangent horizon. The situation is similar to that used constructively in radio occultation GPS receivers where the measurements are processed to obtain tropospheric characteristics. Conversely, in the case of a navigation receiver, usage of such occulted measurements results in position and velocity errors (Fig. 1).

A typical application of navigation GPS receiver in high altitude trajectory vehicles is in aiding the resident inertial navigation system (INS). GPS-INS navigation systems depend on the complimentary accuracy properties of GPS and INS to produce superior performance. The INS errors are slowly varying and unbounded, which can be attributed to sensor drifts, biases and the inherent multiple integration process. Whereas comparatively, GPS errors due to satellite clock and ephemeris parameters, atmospheric propagation, receiver noise and multipath, are all fast varying and bounded generally. The efficacy of the integrated system, based on a complementary filter configuration using an optimal filter such as a Kalman filter, lies in the bounding of the error growth of an INS based system using GPS. Such systems typically have wild input rejection features that protect the complimentary filter internal states from corruption by noisy GPS signal samples. However, the navigation error due to unintentional occultation is of a slowly varying nature, which is uncharacteristic of GPS receivers. Such progressively degrading GPS outputs compromise these usual protection features in the integration scheme, thereby, affecting the states of the filter, resulting in integrated output errors.

A representative simulation case, where a GPS satellite moves into the occulting region, as observed from a GPS receiver in a flight path at an altitude of

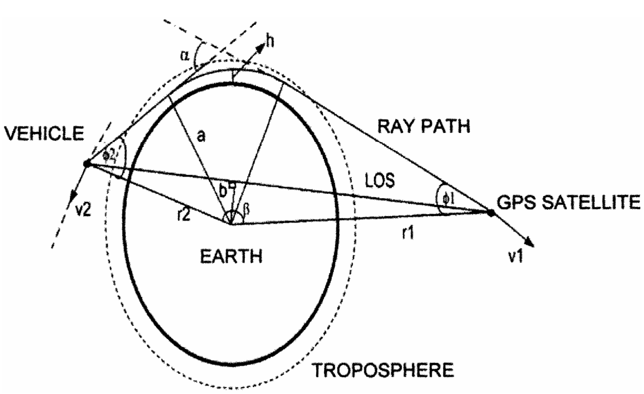

Fig. 1 — GPS receiver in-flight path tracking bent signal

nearly 800 km is presented. The VDOP advantage gained by the use of this 'about to be occulted' negative elevation satellite is quantified vis-à-vis the GPS navigation errors introduced through the continued use of the measurements from this satellite during the occultation period (until signal loss). The effect of these errors on a further downstream uncoupled GPS-INS system is also studied.

An altitude based elevation cut-off scheme that can be incorporated in the GPS receiver for retaining the advantages of using negative elevation satellites, while avoiding occulted measurements is presented. A method for strengthening integration scheme protection, using residuals, for rejecting slow GPS errors is also discussed.

2 Methodology

The GPS receiver is considered to be mounted on a typical high dynamics vehicle. The vehicle flight paths as well as the GPS constellation are simulated using GPS simulator software. Specific choice of flight paths and time of flight are made to obtain scenarios where the GPS receiver has a possibility of tracking an occulted signal from a setting GPS satellite and use it for positioning. Receiver antenna patterns and vehicle maneuvers are incorporated in the simulation to assess realistic GPS satellite visibility. Position and velocities of all the visible GPS satellites, and range as well as range rate measurements as seen by the receiver are logged from the GPS simulator. For the occulted GPS satellite, the tropospheric refraction effect is modeled in Matlab®, and the excess phase and excess doppler are obtained analytically. These values are added to the true (line of sight) range and range rates for the occulted satellite to form the occulted measurements of interest. The receiver measurements and satellite position-velocities are fed into a standard receiver position-velocity computation module based on the least square error (LSE) algorithm. Comparison of the position-velocity solutions including and excluding the occulted measurements reveal the extent of navigation error introduced.

3 Assumptions

The GPS receiver pseudo range measurement is generally different from the true range due to errors from different sources briefed above and is expressed as[1]:

$$\rho_q = r + c[\delta t_u - \delta t^s] + I_q + T + \varepsilon_{\rho q} \qquad \ldots(1)$$

where,

q = L1 or L2 frequency;
ρ = pseudo range measurement;
r = true range from satellite to receiver;
δt_u = receiver clock bias;
δt^s = satellite clock bias;
c = electromagnetic wave speed in vacuum;
I = delay due to ionosphere;
T = delay due to troposphere; and
ε = un-modeled effects & measurement error.

The pseudo range rate measurements are also corrupted by the same sources of error; thereby, yielding a value different from the true range rate. These pseudo range and pseudo range rate measurements from multiple satellites are usually used for navigation computations in standard GPS receivers. However, for the purposes of this study, all the error sources are considered as zero, and true range and range rate from the simulator are utilised to feed into the position-velocity computation algorithm. This allows a clear assessment of the error contributed by the specific situation under consideration. In practice, with selective availability (SA) off, the major source of measurement error is ionosphere; and the assumption of zero ionospheric error is justified to the first order by assuming that the receiver under consideration is a dual frequency GPS receiver that operates on ionosphere free pseudo ranges.

For troposphere, spherical symmetry is assumed, akin to an onion shell. The earth is also assumed to be of spherical shape with a global mean radius of 6371 km. This simplifies computations by allowing the use of Abel integral. Further, the atmospheric refractivity is assumed to be exponentially decreasing with height. This allows simple analytical estimation of the effects on range and range rate measurements from the occulted satellite.

4 Model for tropospheric effect

For modeling tropospheric effects on signals from the occulted GPS satellite, in the form of excess phase and excess Doppler, an analytical approach is used[2,3]. The troposphere is modeled with a bi-exponential refractivity model, consisting of a dry and a wet component, following Kirchengast[2], and is reproduced as:

$$N^{\varphi}(h) = N_d(h) + N_w^{\varphi}(h) = N_{0d} \cdot e^{-h/H_d} + N^{\varphi}_{0w} \cdot e^{-h/H\varphi w} \quad \ldots(2)$$

where,
N_{0d} = dry refractivity component at height h=0
N^{φ}_{0w} = wet refractivity component at height h=0
H = scale height

The subscripts d and w in Eq. (2) represent the dry and wet components, respectively; and φ represents the latitude band. As both the cases discussed in this paper have the ray tangency points located in the equatorial region, the values for the constants are chosen as[2]: $N_{0d} = 287$, $H_d = 7$ km, $N^{\varphi}_{0w} = 86$, and $H^{\varphi}_w = 2.5$ km.

Based on this refractivity model, assuming a spherically symmetric atmosphere, the use of Abel integral yields an analytical bending angle model with respect to height, as derived by Melbourne *et al.*[3] and Kirchengast[2]:

$$\alpha^{\varphi}(h) = a^{\varphi}(h) \cdot N^{\varphi}(h) \cdot (1 + b^{\varphi}(h) \cdot N^{\varphi}(h)) \quad \ldots(3)$$

where,
$a^{\varphi}(h) = 10^{-3} \cdot \sqrt{(2 \cdot \pi \cdot (R_E + h) / H^{\varphi}(h))}$
$b^{\varphi}(h) = 10^{-6} \cdot \sqrt{(2 \cdot \pi \cdot (R_E + h) / H^{\varphi}(h))}$
R_E = mean Earth radius (6371 km)

The model when implemented in Matlab gives a bending angle versus height profile as shown in Fig. 2, and this is independent of the orbit of the satellite and the trajectory of the receiver.

The dependence of bending angle on height is converted into dependence on time using GPS satellite orbit and receiver vehicle trajectory information with a method following the lines elucidated by Sokolovskiy[4] and Zin *et al.*[5]. With three

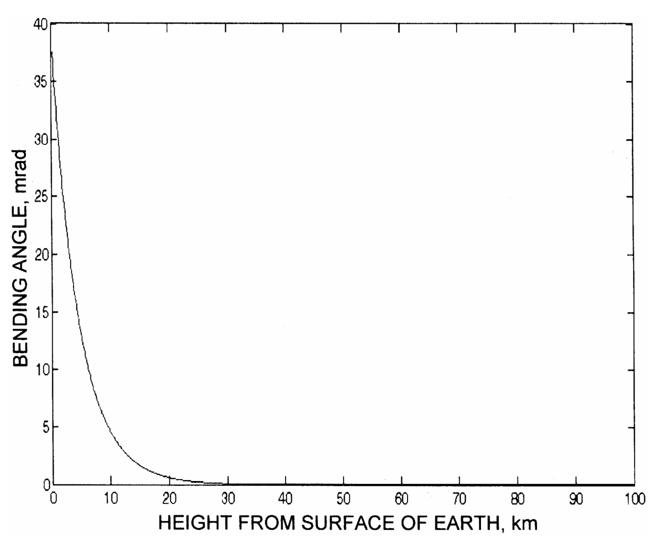

Fig. 2 — Bending angle versus height

constraints, viz. Snell's law at satellite location, Snell's law at receiver location and quadrilateral geometry constraint, given in Eq. set (4), where earth is assumed to be a perfect sphere of radius R_E, an iterative computation is used to obtain the ray zenith angles, Φ1 and Φ2, (i.e. angles between ray tangent and local vertical at the satellite and receiver with position vectors r1 and r2, respectively), and height of tangency point, h, with respect to time from which the bending angle α is obtained. The symbols Φ1, Φ2, α, β, r1, r2, and h are marked in Fig. 1. The refractivity at satellite and receiver locations is assumed to be unity.

$$\left.\begin{aligned} r1 \sin \Phi1 &= R_E + h \\ r2 \sin \Phi2 &= R_E + h \\ \Phi1 + \Phi2 + \beta - \alpha &= \pi \end{aligned}\right\} \quad \ldots(4)$$

With the knowledge of the height of tangency point, and vehicle trajectory, the analytical excess phase model by Kirchengast[2] is used to obtain the excess phase profile with respect to time. The relevant equation set is:

$$L^{\varphi}(h) = (10^{-3}/2)D_L[\,\alpha^{\varphi}(h)\,]^2 + H_d\,\alpha_d(h) + H_w\,\alpha_w(h) \quad \ldots(5)$$

where,

$$D_L = (R_E + h_L)\cos\psi_L;$$

$$\psi_L = \arcsin\left[(R_E + h)/(R_E + h_L)\right]$$

Here, in Eq. (5), h_L, represents the height of the vehicle from earth surface at any instant; D_L, is the line of sight distance between the ray tangency point and the vehicle; and ψ_L, is the angle between position vector of the vehicle and the line of sight vector from vehicle to the ray tangency point.

The knowledge of ray zenith angles, Φ1 and Φ2, allow the unit vectors along the ray to be computed by rotation of the satellite and vehicle position vectors. As the satellite and vehicle velocities are also known, the excess doppler $\delta\rho_{dop}$ is computed as the difference between the doppler along the ray path and along the geometric line of sight[6] as shown in Eq. (6). Here also, the refractive index at both the satellite and the receiver locations are assumed to be unity.

$$\delta\rho_{dop} = T_S . V_1 - T_R . V_2 - V_{12} \quad \ldots(6)$$

where,

T_S = unit tangent vector along ray at satellite;

T_R = unit tangent vector along ray at receiver;

V_1 = satellite velocity vector;

V_2 = receiver velocity vector;

V_{12} = line of sight relative velocity vector between the satellite and receiver; and

'.' represents the vector dot product

The excess doppler can also be directly obtained through numerical differentiation of the excess phase profile with respect to time.

5 Positioning algorithm

Pseudo range measurements from all GPS satellites in view are used to estimate the user receiver position in three dimensions and the user clock bias. As the measurement equations are nonlinear, they are solved by linearizing about an approximate initial value and solving iteratively[1]. The general form of the linear equations are expressed in Eq. (7), where, δw, represents the corrections to the position components; δc, is the correction to estimated bias; δρ, is the difference between the measured and computed pseudo ranges; ε_ρ, represents the error term; and G, is the user satellite geometry matrix.

$$\delta\rho = G[\delta w \;\; \delta c]^T + \varepsilon_\rho \quad \ldots(7)$$

The standard LSE algorithm for over determined solution is utilized to yield minimum sum of squared residuals solution for the corrections as shown in Eq. (8), where ^ represents estimates.

$$[\delta\hat{w} \;\; \delta\hat{c}]^T = (G^T G)^{-1} G^T \delta\rho \quad \ldots(8)$$

The initial estimates are refined through iterations (Newton Raphson method) until the change in the estimates are sufficiently small. Once the user position is determined, the resulting final user satellite geometry matrix can be used in conjunction with the knowledge of satellite velocity and pseudo range rates to obtain user velocity[1] using Eq. (9):

$$\delta\dot{z} = G[v \;\; \dot{c}]^T + \varepsilon_v \quad \ldots(9)$$

In Eq. (9), v, represents the user velocity components; $\dot{c}$, is the user clock drift; $\delta\dot{z}$, is the difference between measured pseudo range rate and the velocity of the satellite projected along the line of sight vector; and ε_v, is the error term. It may be noted that once user position is determined, no further iteration is required in velocity solution.

6 GPS -INS integration scheme

For the purposes of this study, a typical uncoupled GPS-INS scheme is considered as shown in Fig. 3. In this scheme, the functional outputs of the GPS system and the INS system are processed by an integration filter, such as Kalman filter to generate aided outputs[7]. The term 'uncoupled' indicates that there is no feedback. With such an integrated scheme, accuracy improvements of 5 to 6 km in position and tens of ms^{-1} in velocity are usually attained compared to the standalone INS system.

As the INS is a self contained system, whereas GPS depends on external radio frequency signals, well designed integration schemes include protection features to avoid possible corruption of the internal filter states from wild GPS samples. Typically, multiple GPS sample consistency validation, absolute value bound check, position dilution of precision (PDOP) check, etc. are used to screen out bad GPS data. The fundamental premise behind these methods is that GPS errors have only high frequency noise characteristics and do not exhibit slowly varying errors.

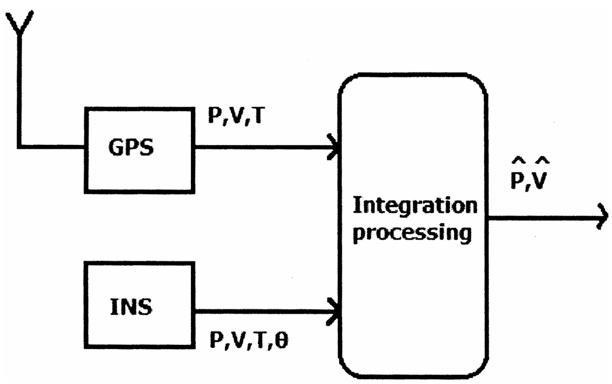

Fig. 3 — Uncoupled GPS-INS scheme

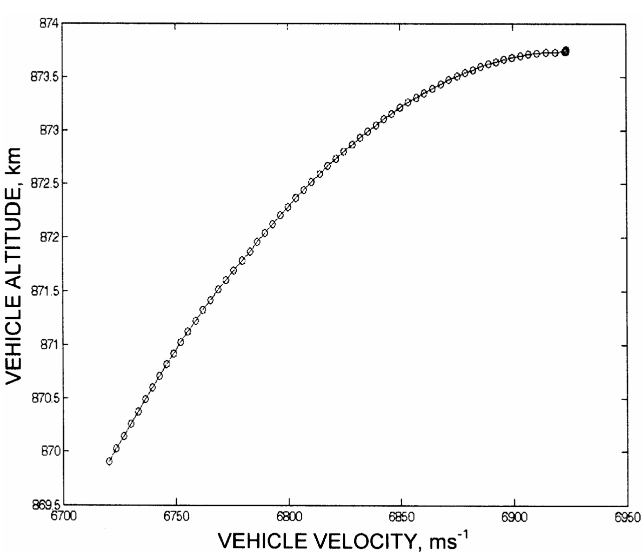

Fig. 4 — Vehicle velocity versus altitude profile

7 Results and Discussion

A typical occultation scenario was generated using Spirent SimGen simulator software. The simulated trajectory is along an arbitrary path at an altitude of nearly 800 km, which is a portion of flight path typically seen during controlled thrusting phase in high altitude vehicles. The altitude versus velocity magnitude of the vehicle for the case is shown in Fig. 4. Considering an eight channel receiver to be used in the vehicle, range and range rate data from eight visible satellites are used for processing, which are depicted in the sky plot of Fig. 5. The '*' indicates those four satellites that yield the best PDOP. The GPS satellite 26 alone is of negative elevation and its trajectory appears moving towards east in the sky plot, whereas all the other satellites are of positive elevation and their trajectories appear moving towards west. As the vehicle advances through the simulated trajectory segment, the negative elevation angle of SVID 26 varies from nearly 22 to 29 degrees, resulting in the satellite being progressively occulted by the earth. With an 'all in view' solution, the

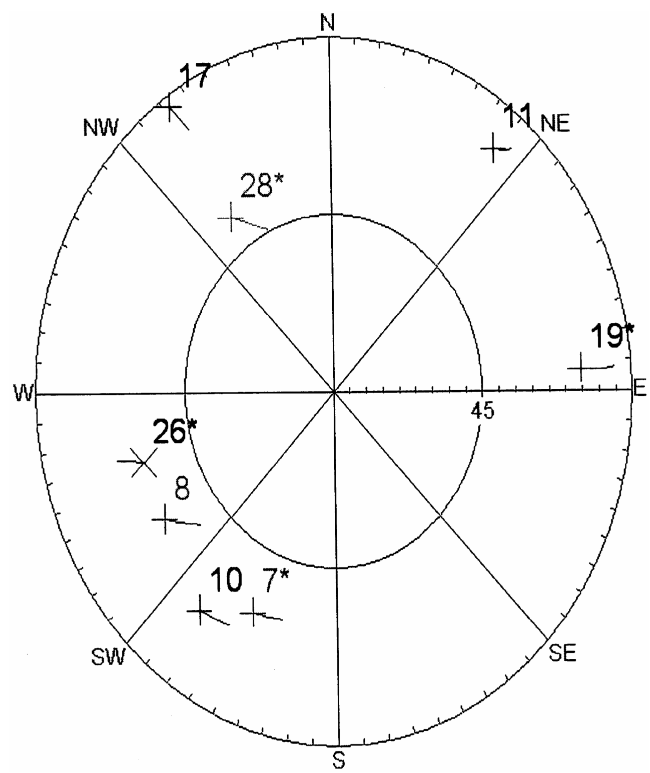

Fig. 5 — Sky plot for GPS satellites used by receiver in-flight

PDOP is 1.41 and VDOP is 1.11, whereas in the case where the occulted satellite SVID 26 is dropped from solution, the PDOP and VDOP are 2.69 and 2.52, respectively. The improvement in DOP is by an order of two, which is the motivation for using negative elevation satellites also in position-velocity computations.

The height of tangency point ‘h’ of the ray connecting this occulting satellite and receiver are computed using the iterative method outlined earlier, and is plotted in Fig. 6 against the geometrical impact parameter (indicated as ‘b’ in Fig. 1). It can be seen that they diverge beyond 40 seconds indicating the onset of occultation, and ‘h’ goes as low as 2 km. For the purposes of clear comparison with ‘h’, in Fig. 6, the geometric impact parameter ‘b’ has been corrected by the earth radius value.

As the satellite sets below the horizon with respect to the receiver, expectedly the bending angle also increases. The bending due to troposphere is seen to be as high as 20 mrad as the height of tangency point reaches near the lowest value as shown in Fig. 7.

Knowing the bending angle due to dry and wet atmospheric components and the height of the tangency point at every instant of the trajectory section, the excess phase model yields values up to 840 m for the case under consideration as shown in Fig. 8.

It is to be noted that the excess phase model includes the effect of propagation velocity change in medium also, in addition to signal bending though the latter is predominant. The computed excess doppler profile is plotted in Fig. 9. Such excess doppler measurements from the occulted satellite are routinely utilized to retrieve atmospheric parameters in GPS radio occultation applications.

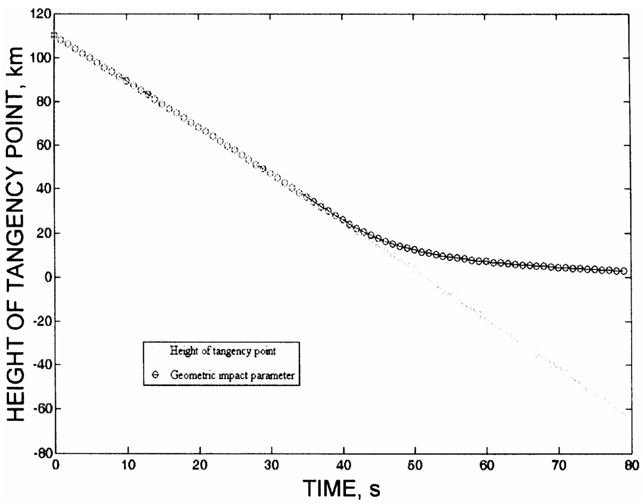

Fig. 6 — Ray tangent point and geometric impact parameter

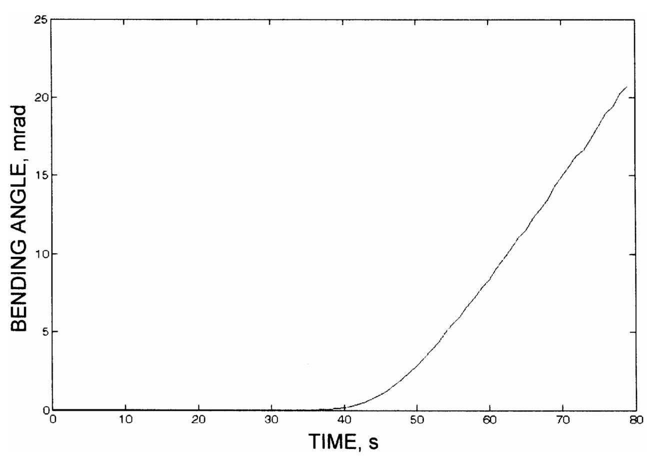

Fig. 7 — Bending angle versus time

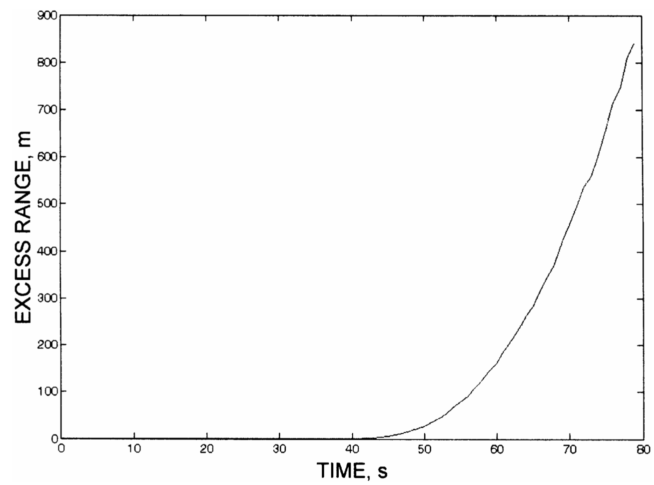

Fig. 8 — Excess phase versus time

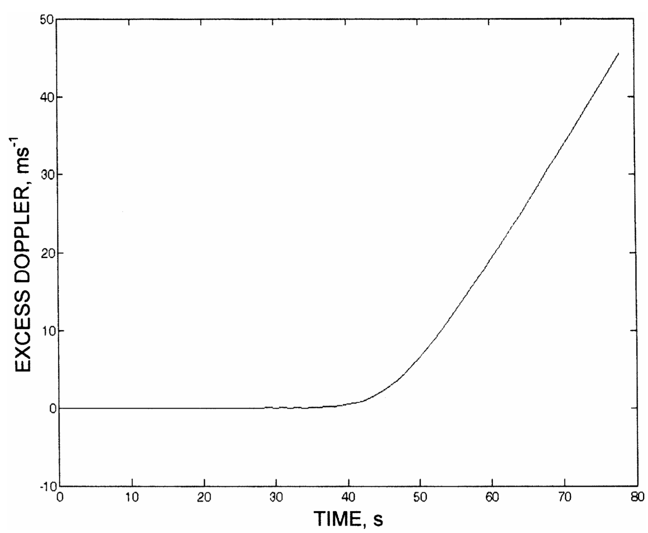

Fig. 9 — Excess Doppler versus time

The excess phase and doppler are added respectively to the line of sight range and range rates to form the range and range rate measurements for the occulted satellite. Position and velocity computations using LSE algorithm with and without the occulted SVID 26 reveals that position and velocity errors of up to 750 m and 38 ms^{-1} in the root mean squared (RMS) sense can be caused by the use of that satellite. This is shown in Fig. 10 and Fig. 11, respectively. It can be seen that though the position velocity solution is formed from eight measurements, the range and range rate error in the negative elevation satellite has a direct and almost one to one bearing on the LSE solution. The impact on the range and range rate error due to the occulted satellite can be reduced in the final solution by weighted LSE approach (weighing based on satellite elevation) but it cannot be eliminated.

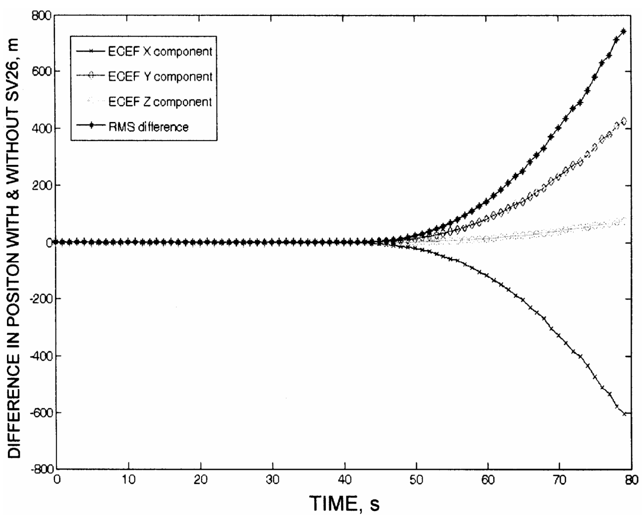

Fig. 10 — Position error due to occultation of SV26

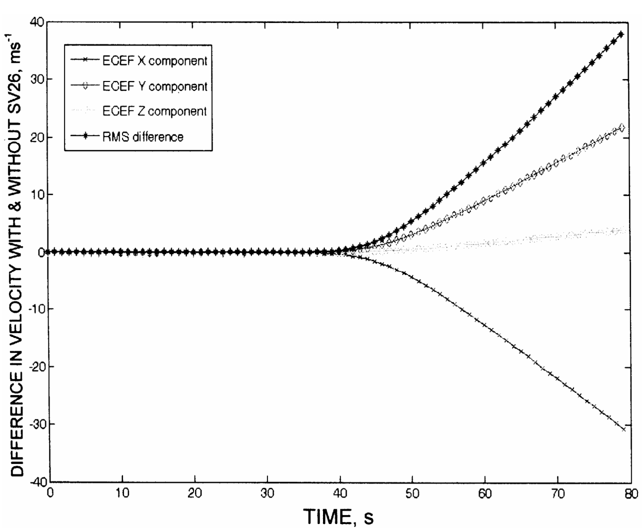

Fig. 11 — Velocity error due to occultation of SV26

However, in practice, the receiver may not continue to track the signal as the height of tangency point reaches very low values because of low signal power. Further, other factors, for example signal acceleration due to high refractivity gradient or physical jerk events on the thrusting vehicle, also may result in early tracking loss. In that case, it turns out to be beneficial for the navigation receiver if it were tracking the occulted satellite, as the position-velocity error will be lower. The tropospheric signal defocusing attenuation is seen to be up to 12 dB in this simulated case, based on the model given by Kirchengast[2], and the attenuation profile with respect to time for this case is plotted in Fig. 12. Based on link budget calculations, a practical phase locked loop (PLL) based receiver with a sensitivity of -145 dBm operating under the conditions of this case will track the satellite with a carrier to noise ratio of 30 dBHz up to nearly 60 seconds beyond which it may lose lock limiting the position error to around 150 m and velocity error to 14 ms^{-1}.

Under such practical GPS error conditions, the effect on the complementary aiding scheme Kalman filter is now discussed. In Fig. 13, it can be seen that the trending in raw GPS velocity results in similar signature in the INS-GPS difference which goes as input to the filter. The resultant corruption of filter is evident from the deviation of estimated states as shown by dotted lines in Fig. 13. GPS velocity error of 14 ms^{-1} in the root sum square (RSS) sense has resulted in an aided velocity error up to 5 ms^{-1} RSS. Correspondingly, the GPS position error of 150 m RSS resulted in aided position error of 100 m RSS.

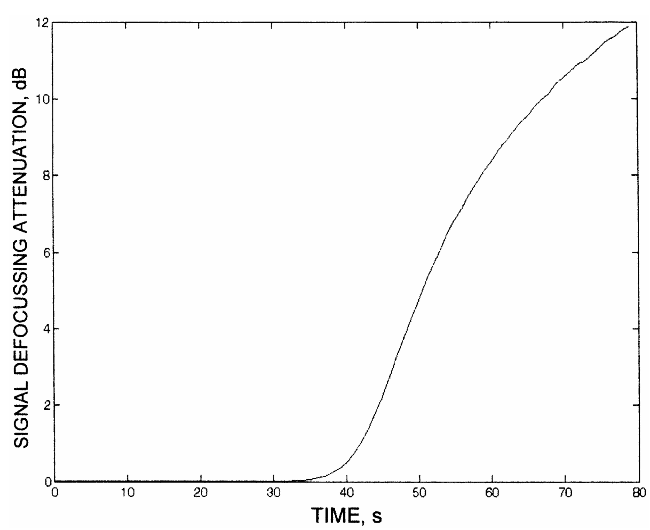

Fig. 12 — Signal defocusing attenuation

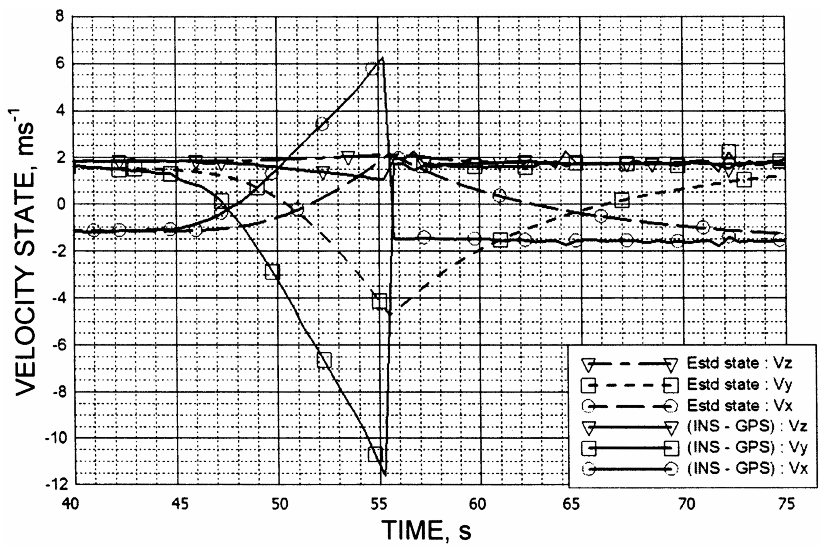

Fig. 13 — Integrated output error due to slowly varying GPS error

8 Error mitigation strategy

The case presented shows that position and velocity errors are progressively introduced in the receiver navigation solution as one of the GPS satellites used in computation sets below the earth horizon. Therefore, it follows logically that the errors can be avoided by forcibly removing that particular satellite from navigation computations from the onset of occultation. Though the actual onset of occultation can be easily identified from the profiles of excess doppler or excess range versus time as in Fig. 8 or 9, it cannot be accurately determined from the measurements in real time as the excess quantities are extremely small in comparison to their absolute values. However, with the knowledge of the vehicle altitude using a spherical earth approximation, the half angle that the earth plus the atmosphere subtends at the vehicle location can be determined. From this angle, a corresponding elevation limit angle can be computed. As the actual elevation of the negative elevation satellite goes beyond this limit value, it can be considered as the onset of occultation, from which point that satellite must be dropped from usage in navigation computations. The satellite receiver geometry for the situation is depicted in Fig. 14. In Fig. 14, V indicates the vehicle position and S indicates the occulted satellite position. The dotted lines with arrow head indicate the vehicle and satellite trajectories; LH, is the local horizontal at the vehicle location; R_E, represents the mean earth radius; h_a, is the assumed height of

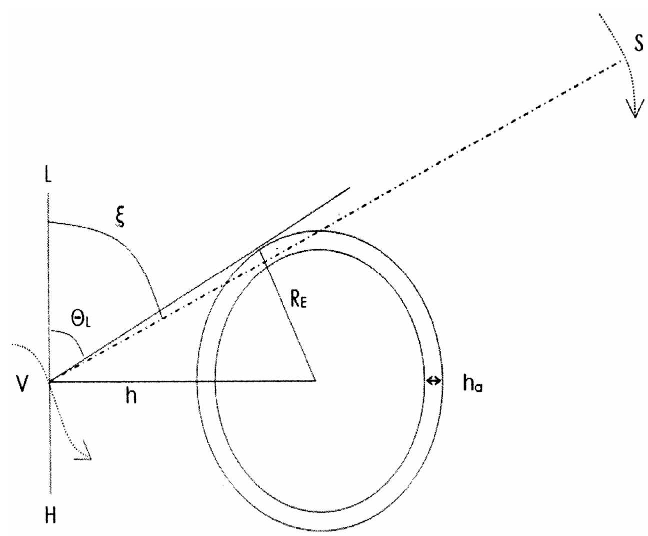

Fig. 14 — Geometry indicating actual elevation angle and limit angle of occulted satellite

the atmosphere; and h, is the actual altitude of the vehicle; ξ and Θ_L, indicate the actual elevation angle and the elevation limit angle, respectively. As an example, the elevation limit angle and actual elevation angle are computed for case under consideration and their magnitudes are plotted in Fig. 15.

In this case, the height of the atmosphere, h_a, has been assumed to be 20 km. It can be seen that beyond 40 seconds, the actual elevation angle to the satellite exceeds the elevation limit indicating the onset of occultation. On comparison of Fig. 8 with Fig. 9, it can be seen that the excess phase and doppler also increases from 40 seconds onwards.

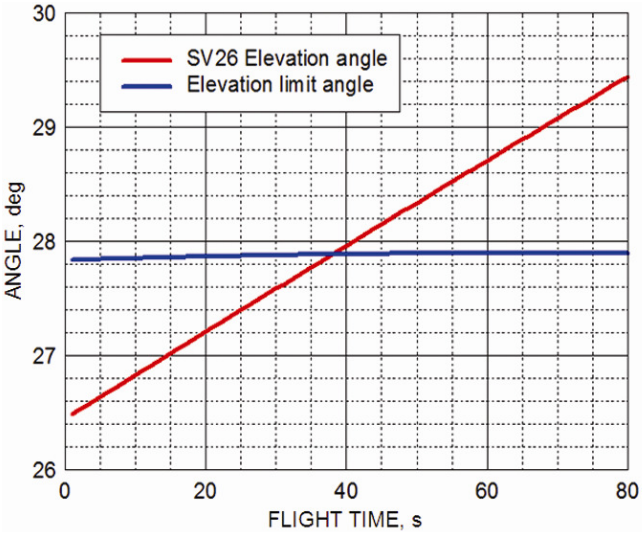

Fig. 15 — Elevation limit angle and actual elevation angle versus profile time

Thus, avoiding the measurements from SV26 beyond 40 seconds, alleviates the possibility of navigation error due to occulted measurements at the same time retaining the DOP advantage due to the negative elevation satellite till that point of time. In practice, the elevation limit angle can be computed assuming a larger h_a so that good margin of 3 to 4 degrees is obtained.

Another aspect of error mitigation is strengthening aiding scheme protection, using GPS-INS residuals, for rejecting such slow GPS errors. This can be implemented as a bound check operating on fixed number of previous samples of residuals. This will avoid the GPS error from affecting the filter states beyond those many samples.

9 Conclusions

In this paper, the effect of troposphere induced navigation output error on GPS receivers in high altitude trajectory vehicles is presented. A case pertaining to typical phase of flight of high altitude vehicles, where error in range and range rate measurement from a negative elevation GPS satellite under occultation due to earth resulted in position and velocity error, is simulated. Results indicate position errors up to 750 m and velocity errors up to 38 ms^{-1}. In practice, the errors vary depending on the atmospheric conditions, vehicle trajectory and the duration for which the receiver maintains lock on the signal from the occulted satellite. In a practical PLL loop based receiver considered, due to loss of lock, the position error is limited to around 150 m and velocity error to 14 ms^{-1}. In the uncoupled GPS-INS scheme studied, GPS error of the above order resulted in integrated system output error of 100 m in position and 5 ms^{-1} in velocity, respectively. An altitude based elevation cut off scheme for utilizing negative elevation satellites is also presented. Under this scheme, the negative elevation satellite is used for positioning until the elevation reaches a computed limit based on altitude, beyond which it is dropped. By adopting this method, the VDOP advantage is retained where as occultation induced errors in navigation solution are completely avoided. A method for strengthening aiding scheme protection, using residuals, for rejecting such slow GPS errors is also presented.

Acknowledgement

The authors express their sincere thanks to Director, ISRO Inertial Systems Unit for his kind support in carrying out this work.

References

1 Misra Pratap & Enge Per, *Global Positioning System: Signals, measurements and performance* (Ganga-Jamuna Press, Lincoln, MA), 2001.
2 Kirchengast G, *A simple analytical atmospheric model for radio occultation applications*, IMG/UoG Technical report for ESA/ESTEC 9 (ESA/ESTEC, Graz, Austria), 1999.
3 Melbourne W G, Davis E S, Duncan C B, Hajj G A, Hardy K R, Kursinski E R, Meehan T K, Young L E & Yunck T P, *The application of spaceborne GPS to atmospheric limb sounding and global climate change monitoring*, NASA/JPL Publ 94-18 (NASA/JPL, Pasadena, California, USA), 1994.
4 Sergey V Sokolovskiy, Tracking tropospheric radio occultation signals from low earth orbit, *Radio Sci (USA)*, 36 (3) (2001) 483.
5 Zin A, Crosta P, Scaciga L & Notarpietro R, *GPS radio occultation from LEO: occultation management and open loop tracking aspects*, Paper presented to 2nd ESA workshop on Satellite Navigation User Equipment Technologies, Noordwijk, 8-10 Dec 2004.
6 Melbourne W G, *Radio occultations using Earth satellites: A wave theory treatment* (John Wiley, Hoboken, NJ, USA), 2005.
7 Vidwani B C, Mohanlal P P, Abdul Shukkoor A & Syamala S, *Aided scheme scheduled gain EKF for data fusion for re-entry navigation*, Paper presented at International conference on avionics systems, RCI, Hyderabad, 21-23 Feb 2008.
8 Sergey V Sokolovskiy, Modeling and inverting occultation signals in the moist troposphere, *Radio Sci (USA)*, 36 (2001) 441.
9 Abdul Shukkoor A, Mohanlal P P & Veeraraghavan P S, *Hybrid navigation system for GNC of space capsule recovery experiment (SRE): Development and flight experience*, Paper presented at 7th International ESA conference on GNC, Tralee, Ireland, 2-5 June 2008.
10 Harikumar G, Karthikeyan K, Syamala S, Radhakrishna Pillai C, Hemachandran S & Mohanlal P P, *Tropospheric effect on navigation GPS receiver performance in high altitude trajectory vehicles*, Paper presented at International Conference in Navigation and Communication (NAVCOM-12), Hyderabad, 20-21 December 2012.